

GaitGuard: Towards Private Gait in Mixed Reality

Diana Romero

dgromer1@uci.edu

University of California, Irvine

Athina Markopoulou

athina@uci.edu

University of California, Irvine

Ruchi Jagdish Patel

ruchijp@uci.edu

University of California, Irvine

Salma Elmalaki

salma.elmalaki@uci.edu

University of California, Irvine

Abstract

Augmented and Mixed Reality (AR/MR) systems offer uniquely immersive and collaborative experiences, fundamentally diverging from traditional mobile interactions. As these technologies become more pervasive, ensuring user privacy is paramount. This paper addresses gait privacy, a critical concern where an individual's walking pattern can inadvertently reveal sensitive personal information like age, ethnicity, or health conditions. We introduce **GaitGuard**, a novel, real-time system designed to safeguard gait privacy against video-based gait profiling threats within MR environments. GaitGuard operates on a multi-threaded framework, incorporating dedicated modules for efficient stream capture, body detection and tracking, and effective privacy protection. Our rigorous evaluation involved testing 248 distinct configurations, systematically varying regions of interest, privacy techniques, and operational parameters. This comprehensive analysis allowed us to thoroughly assess the trade-offs between privacy protection, video quality, and system performance. Furthermore, we propose an innovative adaptive method that intelligently processes only gait-critical frames, significantly enhancing visual quality without compromising privacy for real-time deployment. GaitGuard demonstrates substantial privacy protection, achieving up to a 68% reduction in gait profiling accuracy and inducing a significant feature distribution shift (Jensen-Shannon Divergence of 0.63). Crucially, the system maintains a high performance of 29 frames per second (FPS), ensuring an acceptable user experience. User studies with 20 participants further validate our approach, indicating greater user comfort and acceptance of the privacy-preserving transformations. GaitGuard offers a practical and immediately deployable solution for robust gait privacy in MR, without sacrificing the immersive user experience.

CCS Concepts

- Security and privacy → Domain-specific security and privacy architectures; Privacy protections; • Human-centered computing → Mobile devices.

Keywords

Gait, Mixed Reality, Augmented Reality

1 Introduction

Mixed Reality (MR) has rapidly evolved from research prototypes to mainstream consumer devices, exemplified by sophisticated systems such as the Apple Vision Pro [2], Meta Quest 3 [43], and Meta Aria glasses [44], which build upon foundational platforms like HoloLens 2 [51]. These systems seamlessly blend physical and



Figure 1: Collaborative MR on a shared virtual object: a bystander walks into the headset's view while a remote desktop user assists, exposing moving users to potential video-based gait-profiling attacks.

digital environments, enabling intuitive interaction with virtual objects overlaid on the real world through advanced sensors that provide precise hand-tracking, eye-tracking, and speech input capabilities [52]. These capabilities have opened transformative applications in various critical sectors, including advanced manufacturing processes [23], precision healthcare interventions [65], and immersive educational [75, 77] and collaborative experiences [11, 68, 89].

However, the widespread adoption of MR technologies has raised privacy and security concerns, particularly regarding the potential exploitation of sensor data and camera feeds by passive eavesdroppers to extract sensitive information, including facial information [13], semantic location data [20], camera feeds [82] and sensor data [9, 26, 34, 41, 94]. These privacy challenges are amplified in multiuser MR scenarios, co-located shared physical spaces, and distributed remote collaborations, creating privacy implications for primary users and bystanders within these environments.

This paper focuses on protecting the privacy of the human gait within MR environments. Gait, *i.e.*, the manner of walking, is a recognized biometric identifier that has been used in both medical diagnosis [4] and mobile system authentication [84]. The association of gait data with personal attributes, such as ethnicity [88], age [93], gender [86], and health conditions [73] underscores the importance of its protection. In particular, privacy regulations such as the California Privacy Rights Act (CPRA) [33] and the European Union's General Data Protection Regulation (GDPR) [81] list "gait" as a type of biometric information, which falls under the broader category of "personal information" that is subject to the act's protections.

MR devices equipped with cameras capture environmental context to enable application functionalities but inadvertently collect gait information through continuous recording of user surroundings and movements. This creates a rich data source that potential

adversaries can exploit through **gait profiling**, the process of extracting and analyzing distinctive gait features from captured video footage, to infer personal information about individuals. As illustrated in Figure 1, in collaborative MR scenarios where users work on shared virtual objects, attackers can conduct gait profiling by analyzing captured video footage of both primary users and bystanders who enter the camera view. When combined with advanced machine learning techniques, these extracted gait features can be used to infer individuals' physical and mental health conditions, and predict future [30] behavior. This poses significant privacy risks, particularly for bystanders and others within collaborative MR environments.

This paper seeks to protect gait privacy within the MR domain and makes the following contributions.

- **GaitGuard system design and implementation:** We introduce *GaitGuard*, the first real-time system to mitigate gait privacy compromise in collaborative MR applications susceptible to video-based gait profiling attacks.

- **Assessment of different mitigation strategies:**

We comprehensively examine mitigation strategies suited for MR environments, assessing their performance across various aspects, such as the location of obfuscation (such as lower-body areas), types of obfuscation, and perturbation levels. Our study utilizes privacy and utility metrics relevant to practical MR usage for real-time deployment, delineating the privacy-utility trade-offs presented by different mitigation strategies.

- **Real-time adaptive Defense.**

We introduce a learning-based approach to adaptively identify critical gait events requiring protection, balancing the trade-off between gait privacy protection and computational efficiency for seamless real-time operation in resource-constrained MR environments.

The paper is organized as follows: Section 2 covers the background and related work. Section 3 outlines the threat model. Sections 4 to 6 detail the design and implementation of *GaitGuard*, including mitigation and implementation details. Section 7 evaluates the system, and Section 8 provides practical recommendations. Section 9 concludes the paper.

2 Background and Related Work

2.1 Gait Analysis Methods

Gait analysis is the systematic study of human locomotion, encompassing both walking and running. It characterizes walking as a series of gait cycles, where each cycle (also known as a stride) is defined as the period between successive ground contacts of the same foot. Within this cycle, several critical *gait events* occur, including *toe-off* and *heel strike*, as illustrated in Figure 2.

These gait events form the foundation for extracting *gait features*—quantitative metrics describing temporal and spatial properties of walking [76]. Commonly used features include:

- *Step time (L/R):* Seconds between consecutive bilateral heel strikes.
- *Stance time (L/R):* Seconds from heel strike to toe-off on the same leg.
- *Left and Right Swing time (L/R):* Seconds from toe-off to heel strike on the same leg.

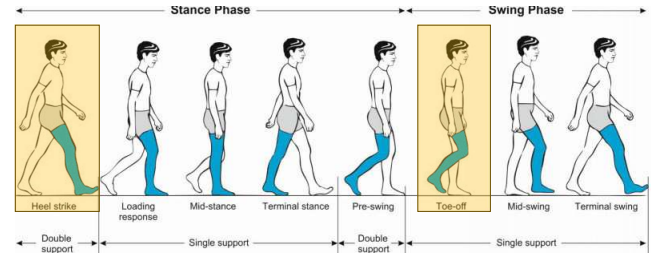


Figure 2: Gait cycle illustration [63]. Critical gait events such as toe-off and heel strike are highlighted.

- *Right to Left and Left to Right Double support time:* Seconds from heel strike of one leg to toe-off of the opposite leg.
- *Step length (L/R):* Meter distance between ankles on heel strike.

Instrumented gait analysis (IGA) is the precise and accurate analysis of gait patterns and characteristics. IGA systems often employ motion capture systems, force plates, walkways, and treadmills [8]. Although this is the gold standard for gait analysis in research practice, these IGA systems are costly and invasive. To address these limitations, researchers have explored alternative, lower-cost sensing modalities for gait analysis, including inertial measurement units (IMUs)[36, 64], gyroscopes[60], and depth sensors such as Microsoft Kinect [21, 61]. More recently, video-based gait analysis using 2D pose estimation has emerged as a compelling solution due to its accessibility and accuracy [39, 76].

In video-based approaches, camera feeds are analyzed using pose estimation algorithms that track the positions of body key points, such as the joints of the head, arms, and legs, over time [35, 90]. Among these tools, OpenPose has become a widely used framework for real-time multi-person pose estimation for video [7]. Studies have shown that the gait features derived from OpenPose can approximate those obtained from IGA systems with reasonable accuracy [76].

In this paper, we focus on video-based gait profiling that uses non-invasive means of extracting gait features from MR-captured camera streams.

2.2 Gait Privacy Beyond Identification

Gait is a well-established biometric identifier that has been widely studied for user authentication in mobile and wearable systems [12, 14, 16, 22], gait offers persistent and passive identification. Unlike passwords or tokens, it cannot be easily concealed or changed [25], making it an attractive target for surveillance and profiling in MR.

However, gait conveys far more than identity. It encodes sensitive attributes such as age, gender, ethnicity, and physical or neurological health [73, 86, 88, 93]. For instance, deviations in gait patterns can indicate early-stage neurodegenerative diseases such as Parkinson's [57] or signal cognitive decline [5]. Unlike facial features or explicit identifiers, these inferences can be drawn unobtrusively, making gait uniquely revealing and difficult to protect. The critical importance of gait privacy extends beyond identification, as demonstrated by real-world cases like actor Billy Connolly. A medical professional "unintentionally" noticed a slight gait alteration, resulting in his Parkinson's diagnosis, underscoring the intimate data contained in our walking patterns [78].

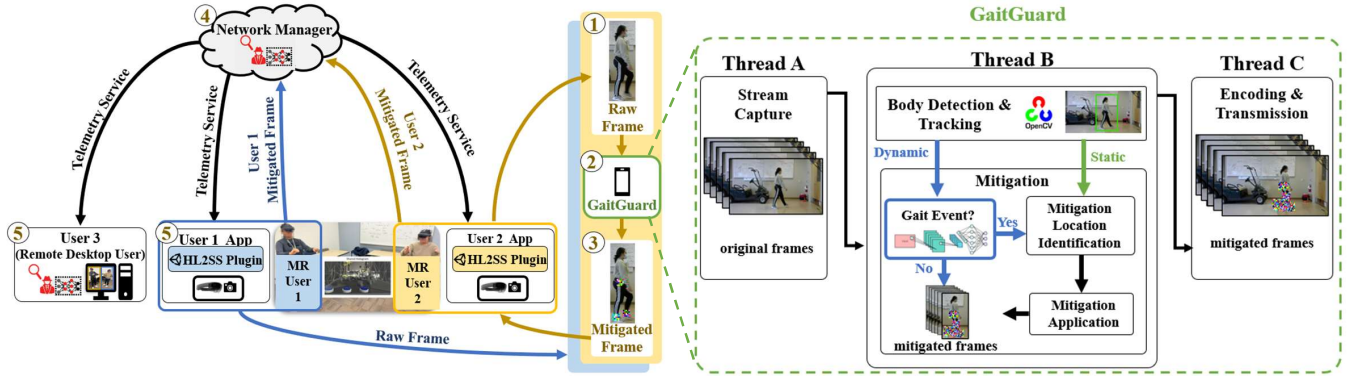


Figure 3: Overview of *GaitGuard*. [Left] Multiple users interact in a collaborative MR app. *GaitGuard*: ① intercepts raw frames from HoloLens 2; ② *GaitGuard* applies gait mitigation; ③ releases mitigated frames to the app—protecting against adversaries on the ④ server or ⑤ remote clients. [Right] *GaitGuard* implemented as three pipelined threads: A captures frames, B detects humans and mitigates gait, C transmits output—maintaining real-time MR performance. An *honest-but-curious* adversary may reside in the telemetry manager or remote desktop client.

Several efforts have explored privacy-preserving methods for gait data in mobile and wearable environments. Techniques include perturbation of inertial measurement unit (IMU) readings [66], obfuscation using distance sensors [83], and anonymization on smartphones [15]. Although effective in controlled scenarios, these approaches assume direct access to user-owned devices and sensors.

MR poses a fundamentally different privacy challenge, as on-board cameras often capture gait data passively from users and unaware bystanders. We focus on *Gait profiling*, which involves extracting distinctive gait features from video footage to infer personal information. Despite the sensitive nature of these data and the ubiquity of head-mounted cameras in MR, no prior work has systematically addressed gait privacy in this context.

2.3 Privacy Vulnerabilities and Defenses in MR

MR devices, equipped with advanced sensors, capture extensive data about users and their surroundings, including video, audio, and motion information. This data collection poses risks not only to users but also to non-consenting bystanders and passersby. MR environments have privacy issues ranging from visual data risks to spatiotemporal security [9]. Past works have highlighted the vulnerability of visual data in MR settings [1, 27], and while solutions like privacy markers have been proposed, they require user compliance and do not protect bystanders [67]. Perceptual manipulation attacks (PMA) can alter user perceptions in collaborative MR environments, compromising secure interactions [10]. In addition, sensor-based side-channel attacks have emerged across immersive platforms. These include inferring keystrokes using infrared tracking [91], controller acoustics [41], and extracting speech from zero-permission motion sensors [34].

These findings underscore the potential for sensitive behavioral and biometric data leakage in immersive systems. Some efforts, such as BystandAR [13], have focused on protecting facial privacy. However, the protection of gait privacy in MR environments remains largely unexplored, presenting a gap in current research and privacy protection measures.

3 Threat Model

Collaborative MR applications introduce novel privacy challenges due to their networked and distributed architecture. Unlike traditional single-user applications, these systems rely on real-time data streaming between users and remote servers, creating multiple points of potential data interception and analysis. Privacy risks are exacerbated by (i) the reliance on camera access for core MR functionalities, such as avatar rendering and environmental interaction, and (ii) the interconnectedness, where data traverses multiple entities and devices. Our analysis of 318 HoloLens applications revealed that 26% request camera access, underscoring widespread exposure to gait profiling within deployed MR systems.

The Collaborative MR Environment. Consider a typical collaborative MR session, depicted in Figure 3. A user wearing an MR headset, such as the HoloLens, captures camera and sensor data streams to facilitate immersive interaction. These applications typically involve local processing on the MR device, followed by transmission of raw or processed data over a network to a network manager. This network manager acts as a central hub, synchronizing and redistributing telemetry data, including rendered video feeds or abstracted information to other participants in the session.

The networked architecture opens avenues for eavesdroppers and “honest-but-curious” entities¹ at various points in the network path to conduct gait profiling attacks from transmitted camera frames. We consider two primary attackers based on their location and role within the networked MR application.

Attacker 1: Operator of the Central Synchronization/Relay Service: Many collaborative MR applications utilize a central server or cloud-based service, such as Photon Network Manager [18], to facilitate real-time synchronization of user states, shared environments, and potentially raw or processed sensor data. An operator of this service, whether the application developer or a third-party provider, has privileged access to data as it passes through their infrastructure. This central point of data aggregation in a common MR architecture presents an opportunity for an honest-but-curious operator

¹ Honest-but-curious attackers comply with MR protocols yet mine accessible camera feeds for sensitive private data.

to observe and potentially log and extract gait-related information from multiple users' data streams.

Attacker 2: Remote Collaborating User. Participants in a collaborative MR session typically exchange data directly or indirectly. A remote user receives updates about other users, which often include avatar representations driven by their movements and shared camera streams from co-located users with head mounted devices (HMD). A curious remote user can passively record and analyze these received data streams to infer the gait patterns of other participants. The inherent data sharing mechanisms in collaborative MR applications, necessary for shared experiences, expose gait information to remote users.

Attacker Capabilities and Goal. Regardless of the attacker's role in the MR architecture, we assume they have *access* only to camera frames captured by the MR device during collaborative sessions containing individuals walking. As discussed above, this access is possible at various points in the network, including: (i) back-end infrastructure (e.g., central server or cloud-based service), or (ii) rendered streams to remote users (i.e., users on laptops, not MR headsets). Although MR systems may incorporate other sensor modalities such as IMU data, eye tracking, audio, or depth maps, we do not assume access to these. The attacker's *goal* is to infer the distinctive gait features of individuals captured in the RGB camera stream, whether they are users of the MR application or bystanders, through video-based gait profiling.

Attack Characteristics. This threat is realistic due to the networked nature of collaborative MR, which continuously transmits camera feeds to enable shared perception, remote avatar control, and annotations. Unlike threats requiring physical proximity, malicious software, or compromised devices, this model relies solely on legitimate access to camera frame data during normal MR operations. Furthermore, given the typical duration of human gait cycles lasting 1~1.3 seconds [62], attackers can readily collect enough visual data to profile gait patterns. These attacks are stealthy as users cannot monitor how their movement data is managed across the network. Although large-scale gait privacy attacks in MR may not currently be a dominant threat, they represent a growing concern with significant potential. As MR adoption increases², the likelihood and sophistication of gait privacy attacks will increase, requiring solutions for privacy-preserving MR systems.

Proposed Defense. To address the unique challenges of gait privacy in networked collaborative MR environments, we propose *GaitGuard*, a companion application on a trusted and paired mobile device. It intercepts video frames and applies lightweight privacy-preserving transformations in real-time. Furthermore, it operates on video frames at their source, mitigating risks from multiple attacker types (central server and remote user). By balancing privacy protection with real-time performance requirements, *GaitGuard* aims to safeguard gait information while maintaining core MR functionality. To the best of our knowledge, no prior work provides real-time defense for camera streams specifically targeting gait privacy, considering the comprehensive mitigation space we explore (i.e., 248 configurations with adaptive strategies).

²The MR market, valued at \$1.4 billion in 2023, is projected to double by 2030 [38].

4 GaitGuard System Design

GaitGuard design focuses on obscuring gait features while preserving visual quality using a paired mobile device to process MR headset video frames, as illustrated in Figure 3. *GaitGuard* balances privacy protection with real-time performance.

4.1 Design Constraints

Building *GaitGuard* for real-world MR systems presents several unique challenges. First, video transformations must preserve essential visual content required for MR functionalities such as spatial mapping, QR code detection, and avatar rendering. Excessive distortion can degrade the user experience and impair collaboration. Second, commercial MR headsets, such as the HoloLens 2, have limited computational resources and operate within tightly restricted platforms. These systems restrict low-level access to camera streams, making on-device interception and transformation infeasible. These hardware and software limitations require innovative approaches to implement effective privacy-preserving measures in MR environments.

4.2 Architecture and Deployment Strategy

Although direct in-headset transformation of gait-related features would provide the most seamless protection, current commercial platforms do not support such access. For example, HoloLens 2 runs Windows Holographic OS, a closed platform that prevents developers from intercepting or modifying raw camera streams [50]. Similar limitations have been encountered in prior work on MR privacy, such as BystandAR [13], which also relied on third-party application processing to enforce privacy protections.

Moreover, the computational cost of video-based gait analysis renders it impractical for real-time execution on current MR headsets. For example, running OpenPose, a widely used pose estimation framework, achieves only 11 frames per second (fps) on a high-end Nvidia V100 GPU, and less than 1 fps on a standard CPU [6]. These rates do not reach the 30 fps needed for smooth real-time MR capture [48].

To address these challenges, *GaitGuard* is designed to offload privacy processing to a companion mobile device. Camera frames from the MR headset are streamed in real time to the mobile device, where gait detection and mitigation are applied. The transformed frames are then returned to the MR application pipeline. This design enables low-latency operation while avoiding the limitations of headset compute power and OS restrictions. It also offers broad compatibility with existing MR systems, allowing deployment without modification to the headset firmware or applications.

4.3 Assessment of Gait Profiling Feasibility

Before developing mitigation techniques, we first evaluated the extent to which gait features are exposed through egocentric video captured by MR headsets. To this end, we built *GaitExtract*, a lightweight gait profiling tool adapted from the clinically validated approach by Stenum et al. [76], utilizing keypoints from OpenPose.

As illustrated in Figure 4, *GaitExtract* is specifically tailored to the challenges posed by head-mounted MR footage. Unlike fixed-camera settings, egocentric video introduces dynamic perspectives, variable body poses, and partial occlusions, all of which complicate

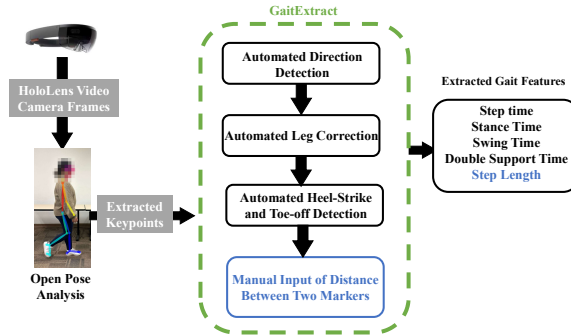


Figure 4: *GaitExtract*: An egocentric MR gait-profiling pipeline using OpenPose to extract temporal features and estimate step length with minimal calibration.

gait profiling. To address these issues, *GaitExtract* incorporates several MR-specific adaptations:

- Estimating walking direction from moving, egocentric viewpoints.
- Correcting leg-side misclassifications due to noisy or occluded keypoints.
- Detecting gait events (e.g., heel-strike, toe-off) in unconstrained, real-world sequences.
- Filtering incomplete or corrupted gait cycles from brief or interrupted video segments.
- Aggregating gait metrics across valid walking intervals.

GaitExtract supports two analysis modes: fully automated and partially automated. The fully automated mode extracts time-based gait features, excluding spatial metrics such as step length. In contrast, the partially automated mode includes step length estimation, but requires minimal manual calibration input. These two modes offer flexibility in gait profiling, allowing for comprehensive feature extraction with varying levels of user intervention.

For each walking sequence, which refers to a video instance of a participant walking in one direction, the tool outputs a ten-dimensional feature vector per leg, including step time, swing time, stance time, and double support time. These extracted features from *GaitExtract* are used as ground truth to evaluate the effectiveness of our gait mitigation strategies, as they rely on a clinically validated approach [76].

4.4 Mitigation Design Aspects

We developed a set of mitigation strategies to obscure gait profiling in egocentric MR video. These strategies span four primary design aspects: ❶ **location**, ❷ **size**, ❸ **type**, and ❹ **adaptability**, as summarized in Figure 5.

❶ Location – Where to Apply Mitigation. We explore spatial targeting of mitigation based on two approaches: keypoint-based masking and region-based masking.

• **Keypoint-Based Masking (KPM).** Inspired by prior work identifying specific anatomical landmarks as critical for gait recognition [76], we evaluated several configurations of keypoint masking:

- (1) **KPM (baseline):** Masks regions surrounding three core gait-related keypoints—midhip, left ankle, and right ankle to directly disrupt the detection of heel strike and toe-off events.

- (2) **Head and shoulders KPM:** Expands the masking to include head and shoulder joints, exploring whether concealing upper body movement enhances privacy while preserving leg visibility.
- (3) **Lower body KPM:** Focuses exclusively on lower body joints, including hips, knees, heels, and toes, which are most indicative of gait patterns.
- (4) **All-except-head KPM:** Masks all body keypoints except the head, offering maximal gait-related obfuscation while retaining facial context for MR interaction tasks.

• **Lower Body-Based Masking (LBM).** In clinical gait assessments, lower body motion is often the primary focus [42]. Building on this principle, we implement a region-based strategy that masks the entire lower body using a bounding box. This method is conceptually similar to lower body KPM, but avoids per-keypoint computation by directly covering the anatomical region, reducing processing overhead while maintaining coverage of gait-critical areas.

❷ **Size – Area of Keypoint Masking.** To balance privacy protection with visual quality, we varied the masked region size around each keypoint. As shown in Figure 5, increasing mask size provides greater concealment of gait-relevant body parts, but also introduces more distortion in the frame.

For the KPM baseline approach, we evaluated the box sizes of 50, 100, 150, and 200 pixels to ensure adequate coverage of spatially dispersed keypoints. For the other variants of KPM (e.g. head and shoulders, lower body, all-except-head), we tested box sizes of 50, 100 and 150 pixels.

In contrast, the Lower Body-Based Masking (LBM) approach uses a fixed-size bounding box that encompasses the entire lower body region. Since it does not rely on individual keypoints, it does not support variable mask sizing, prioritizing simplicity and computational efficiency over fine-grained control.

This exploration of mask size highlights the trade-off between visual quality and privacy strength, which informs configurations based on the context of the application and the sensitivity of the data being captured.

❸ **Type – How to Obscure Gait Features.** Numerous methods have been proposed to reduce privacy risks in camera-captured data, including adversarial perturbations [87], GAN-based anonymization [71], imperceptible privacy filters [70], and quantization techniques [32]. However, many of these approaches are computationally intensive and unsuitable for real-time MR applications. In particular, prior work on applying adversarial perturbations to real-time video frames has found that such techniques are much too computationally intensive to run online [24]. Furthermore, most adversarial protection mechanisms require class-specific training, which limits their generalizability to unseen classes [79, 92]. Therefore, in our work, we deliberately evaluate feasible lightweight mitigation techniques under **real-time** constraints. The mitigation types we explored are as follows:

- **Black Box.** Inspired by the BystandAR system [13], this approach places a solid black rectangle over the gait-relevant regions. It serves as a baseline technique because of its simplicity and guaranteed concealment, although it introduces high visual distortion.
- **Differentially Private Pixelization (DP Pix).** Adapted from Fan et al. [19], this method ensures differential privacy by pixelizing regions and adding noise to the resulting blocks in grayscale images.

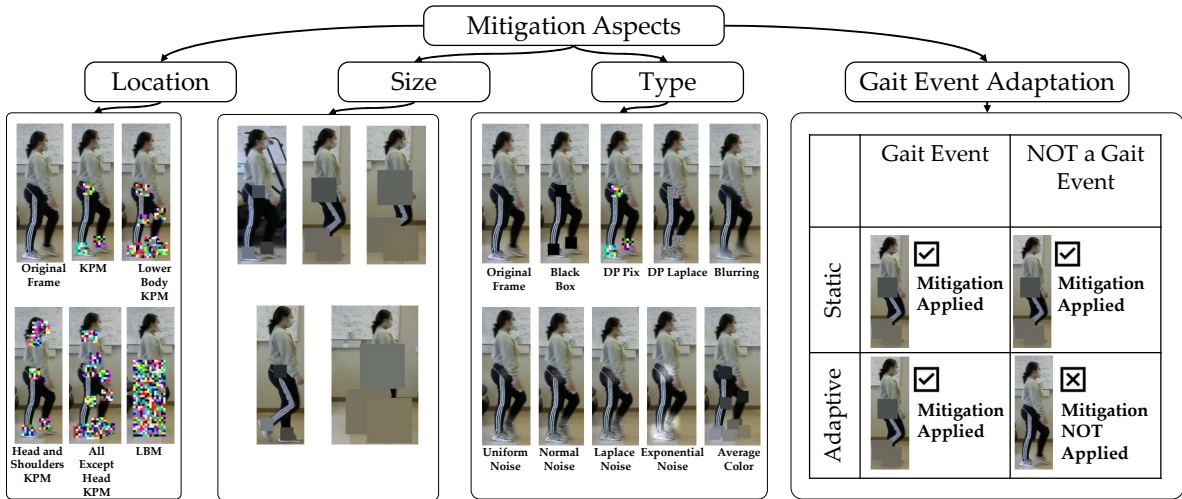


Figure 5: Design space of gait mitigation strategies in MR. Mitigation techniques are explored along four aspects: ❶ location of application, ❷ mask size, ❸ type of transformation, and ❹ adaptability. Each axis presents trade-offs in privacy protection, visual quality, and computational efficiency.

We extended it to RGB by applying noise to each color channel separately. The process involves:

- (1) Determining m , the number of pixels in the target region (based on keypoints or the lower body).
- (2) Applying pixelization using a kernel of size $b \times b$.
- (3) Adding Laplace noise to each pixelized cell, with scale parameter $\lambda = \frac{3 \cdot 255 \cdot m}{b^2 \cdot \epsilon}$.

For KPM, $m = \text{keypoint_count} \cdot \text{box_length}^2$, using up to 25 Open-Pose keypoints. For LBM, m corresponds to the entire lower body area. We tested kernel sizes $b \in \{10, 20, 30, 40, 50\}$ with $\epsilon = 0.1$.

- *Differentially Private Laplacian Noise (DP Laplace)*.

The method applies Laplace noise to each pixel directly, avoiding pixelization:

- (1) Selecting m target pixels within k critical regions.
- (2) Calculating global sensitivity Δf based on k and m .
- (3) Adding Laplace noise to each of the m pixels, scaled by $\lambda = \frac{\Delta f}{\epsilon}$.

We tested values of $\epsilon \in \{0.1, 10, 100, 1000\}$. For LBM, we set $k=1$ and m to all pixels within the lower body region.

- *Gaussian Blur*: Blurring is widely used to obfuscate sensitive information in videos, such as YouTube’s face-blurring feature [85]. We applied a Gaussian blur with a kernel size of $c \times c$ and standard deviation $\sigma=0$, evaluating $c \in \{5, 25, 45, 65\}$.

- *Random Noise*: Our main motivation is finding a lightweight mitigation strategy to achieve a good privacy-utility tradeoff. Hence, we also evaluated simple random noise within the masked regions defined by KPM or LBM using four distributions: uniform, normal, Laplace, and exponential. Each variant used a Hanning window to produce smooth edges. The noise intensity was controlled by a distribution parameter $\lambda \in \{50, 100, 150, 200\}$ as follows: (1) Uniform: Range $[-\lambda, \lambda]$, (2) Normal: Standard deviation λ , (3) Laplace: Scale parameter λ , and (4) Exponential: Rate parameter λ .

- *Average Color*: This method replaces each masked segment with its mean RGB color, maintaining the scene’s overall context. It provides a simple and efficient means to obscure regions pertinent to gait.

Mitigation Combinatorics. Across the three mitigation aspects, including spatial location (❶), mask size (❷), and type of transformation (❸), we evaluate a total of *248 unique combinations* of mitigation techniques. These include 112 DP-Laplace, 68 DP-Pix, 8 Gaussian blur, 32 additive noise, and 28 average color and black-box settings, each reflecting valid combinations of transformation-specific parameters, layout-size variants, and, where applicable, λ levels. This comprehensive design space enables systematic analysis of privacy-utility trade-offs and guides the selection of optimal strategies for deployment in MR environments.

5 Adaptive & Lightweight Mitigation

The mitigation strategies described in Section 4.4 are applied uniformly to all video frames, a mode we define as *static mitigation*. Although effective, this approach can be resource-intensive and degrade both visual quality and processing performance. To address this, we explore the dimension of **adaptability** (❹) by introducing an *adaptive mitigation* strategy—one that selectively applies transformations only to frames containing gait-relevant information. This lightweight mechanism improves visual quality and system efficiency while preserving gait privacy.

Important Gait Events Detection. To develop an adaptive method that maintains privacy guarantees, it is essential to identify which frames contain relevant gait information and which can be processed without mitigation. Based on gait cycle theory, we propose that gait profiling information is critical during two specific phases: heel strike and toe-off events. These are recognized as the most informative gait events, as most gait profiling features depend on the timing and characteristics of toe-off and heel strike events for both left and right legs [63]. Therefore, we define these heel strike and toe-off phases as “important gait events” and propose applying mitigation selectively, particularly only to frames containing these critical events while leaving other frames unmodified.

Dataset Creation. No existing dataset provides labeled visual data for distinguishing gait events from non-gait events in classification tasks. To address this gap, we created a novel labeled dataset

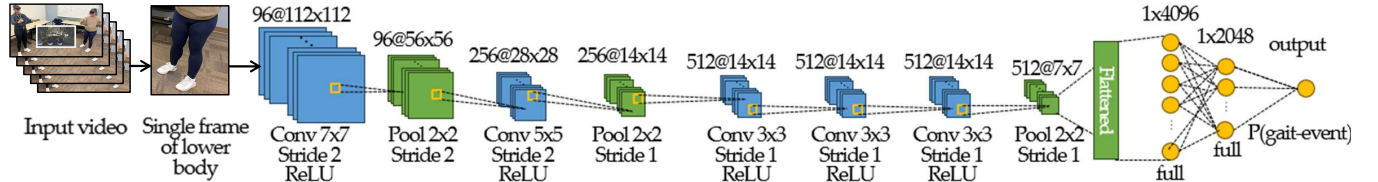


Figure 6: Spatial ConvNet architecture for classifying gait events, providing the likelihood of a frame containing a heel strike or toe-off event.

that differentiates gait event frames (frames showcasing heel strike and toe-off events) from non-gait event frames, derived from 1,197 walking sequences of 20 users recorded using the HoloLens 2. We developed our own labeling methodology by adapting the video-based algorithm and clinically validated approach of Stenum et al. [76] for identifying heel-strike and toe-off in videos. Our labeling strategy includes frames immediately before, during, and after heel-strike or toe-off events to capture the full temporal context of gait transitions. The dataset focuses on the lower body region of users, identified by utilizing YOLOv5 [28] for person detection and cropping the lower half of the bounding box. Our dataset reflects the natural distribution of gait and non-gait event frames across all collected data, providing a foundational resource for training gait event classification models.

Gait Event Classifier. To enable adaptive identification of gait events in real-time MR applications, we designed and implemented a custom convolutional neural network (ConvNet) that identifies frames associated with gait events by learning spatially relevant patterns unique to heel-strike and toe-off phases. Our initial approach explored a two-stream architecture with separate pathways for spatial learning (RGB input) and temporal learning (optical flow input), recognizing that gait events exhibit both spatial visual characteristics and temporal dependencies within the gait cycle. However, our experimental analysis revealed that while the temporal stream provided marginal performance improvements, the real-time computation of optical flow introduced significant latency that compromised streaming performance in MR environments. Consequently, we optimized our design to a single spatial ConvNet that maintains high accuracy while meeting real-time constraints.

Our final ConvNet architecture comprises five convolutional layers, two fully connected layers, and an output layer which represents the probability that the input image is a "gait-event" where the inputs are the RGB crops of the lower body region. This architecture is summarized in Figure 6. The network outputs a single probability p , and we apply a 50% threshold: if $p > 0.5$, the frame is labeled as a gait-event; otherwise, it is labeled as not-gait-event. This threshold is selected to maximize recall, ensuring that all actual gait events are detected, even at the risk of allowing some false positives. To address the inherent class imbalance in gait data, where gait events constitute only a small fraction of walking sequences, we employed the Focal Loss function proposed by Lin et al. [37], defined as:

$$FL(p,y) = -\alpha y(1-p)^\gamma \log(p) - (1-\alpha)(1-y)p^\gamma \log(1-p), \quad (1)$$

where p is the model's predicted probability of the image being a gait-event and y is the ground truth label where 1 represents gait-event frames and 0 represents non-gait-event frames. Through

systematic hyperparameter optimization, evaluating γ values of 2 and 2.5, and α values of 0.7, 0.75, 0.8, 0.85, and 0.9. This process revealed that $\alpha=0.8$ and $\gamma=2.5$ yield the best performance, achieving a recall rate of 94.3% in classifying gait events.

6 GaitGuard System Implementation

GaitGuard system is deployed as a companion application written in Python, running along with an MR application on the HoloLens 2. The system consists of a multi-threaded, pipelined architecture, with each processing stage handled by a dedicated thread to ensure high throughput and real-time performance. *GaitGuard* is illustrated in Figure 3.

Companion Application. The companion application is paired with the Microsoft Multi-user Mars Rover Application [47], the baseline architectural framework for multi-user applications on the HoloLens 2. The application is configured to stream camera frames from the HoloLens 2 to the *GaitGuard* server. This design ensures that *GaitGuard* can be integrated into a wide range of existing and future multi-user MR applications with minimal modification.

Pipelined Thread Architecture. *GaitGuard* system is designed around a pipelined processing architecture with four major modules, running in separate threads: *Thread A* which handles stream captures, *Thread B* which handles body detection and mitigation, and *Thread C* which handles encoding and transmission. These threads communicate via shared queues, allowing each stage to operate independently and asynchronously for real-time performance.

- *Stream Capture Module (Thread A).* This module receives raw video frames from the MR headset. It uses HL2SS APIs to establish a connection and configure stream parameters, including resolution, frame rate, and codec. Once connected, it continuously captures frames and adds them to the `original_frames_queue`. Operating in its thread, this module is isolated from processing delays in downstream modules, enabling uninterrupted frame acquisition from the headset.

- *Body Detection & Tracking and Mitigation Module (Thread B).* This thread combines two modules that process incoming frames to detect the human body and apply privacy-preserving transformations. Human body detection uses OpenCV's Histogram of Oriented Gradients (HOG) descriptor with a pretrained SVM classifier [59]. To reduce processing time, frames are resized to 320x240 and converted to grayscale.

For gait-profiling mitigation, this thread applies the strategies described in Section 4.4. In the KPM approach, OpenPose is used to locate key points, such as the hips, ankles, and knees, and targeted mitigation is applied to these regions. In LBM, the lower half of

the detected bounding boxes is treated as the region of interest and masked accordingly.

Mitigation is applied statically or adaptively as explained in Section 5. The processed frames, with selected mitigation applied, are then reassembled and placed in the `mitigated_frames_queue` for encoding.

- *Encoding & Transmission Module (Thread C)*. This module retrieves mitigated frames from the queue, compresses them, and transmits them to the MR system. To reduce bandwidth, frames are resized to 30% of their original resolution and encoded using JPEG with a quality setting of 10. This compression balances visual quality and transfer efficiency. Transmission is handled via a UDP socket configured for high-throughput streaming. Running in a dedicated thread, this module ensures that encoding and network operations do not interfere with upstream frame capture or mitigation, sustaining the system’s real-time capabilities.

By structuring *GaitGuard* as a multithreaded pipelined system, we maintain a steady frame rate and minimize latency across the capture, analysis, mitigation, and transmission stages. This architecture enables deployment in real-time MR applications. Critically, the mitigation process occurs on background-processed frames within the network manager, without affecting the user’s camera view (egocentric view) or virtual objects.

7 Evaluation

We evaluated *GaitGuard*’s capability to reduce gait profiling while preserving real-time and visual quality in collaborative MR applications. Our study tested 248 strategies in static and adaptive modes (Section 4.4), assessing privacy, utility, and system performance.

7.1 Evaluation Methodology

We implemented *GaitGuard* as a companion system for a collaborative MR application on HoloLens 2. The mitigation module runs on a Samsung S23 Ultra Android phone.

Data Collection. We conducted an IRB-approved user study with 20 participants (aged 18 +), recruited via mailing lists and referrals. To protect identity, participants wore face masks to prevent facial recording, and all data collected was anonymized. Participants walked between two markers (2.5m–2.75m apart) for approximately 5 minutes while being recorded using the HoloLens 2 camera (Figure 7). This setup reflects natural MR collaboration settings that involve limited user movement.

Our participant count aligns with prior research on AR bystander privacy (e.g., 16 participants in BystandAR [13]). The goal was not to build a gait dataset but to evaluate the feasibility of gait profiling attacks and mitigation in typical MR use cases.

Evaluation Metrics for Mitigation Effectiveness. To measure the impact of each mitigation strategy on gait profiling, we applied the 248 configurations described in Section 4.4. We used the fully automated version of *GaitExtract* to extract gait features from unmodified and mitigated video frames. This simulates a realistic adversarial scenario where the attacker has limited resources and no manual calibration access.

- *Privacy Metrics*. Let G represent the gait feature vectors from original frames and G' those from mitigated frames. We evaluated privacy protection using the following metrics:

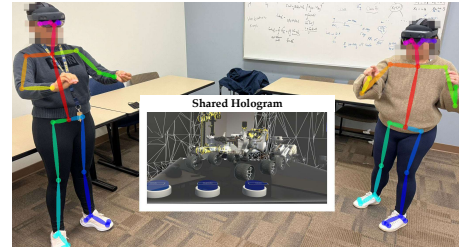


Figure 7: Data collection setup for recording walking sequences using the HoloLens 2 within a collaborative MR application.

- (1) *Jensen-Shannon Divergence (JSD)*: Measures the statistical difference between the distributions of G and G' , quantified as a value between 0 and 1. A higher JSD indicates greater distortion of gait features.
- (2) *Mann-Whitney U Test*: A non-parametric test to determine whether G and G' come from the same distribution. A p-value < 0.05 indicates significant differences, suggesting effective mitigation.
- (3) *User Gait Profiling Accuracy*: Evaluates how accurately individuals can be profiled based on their gait features by comparing the accuracy of the user’s gait features in G' to those in G . Lower accuracy after mitigation indicates improved privacy.
- *Utility Metrics*. To assess visual quality after mitigation, we use the following metrics:
 - (1) *Peak Signal-to-Noise Ratio (PSNR)*: Evaluates the level of distortion introduced across RGB channels.
 - (2) *Structural Similarity Index (SSIM)* [58]: Quantifies perceived visual quality difference by comparing luminance, contrast, and structure between original and mitigated frames.

Cross-Validation with Multiple Gait-Analysis Methods. To assess the robustness of the most effective mitigation technique, we evaluated it against two gait analysis pipelines: (1) our adapted *GaitExtract* based on OpenPose, and (2) GaitLab [29], a gait analysis framework based on deep learning. While *GaitExtract* uses numerical estimation of gait events, GaitLab extracts features using a neural network. The evaluation of both provided complementary information on how resilient our mitigation is against traditional and ML-based gait analysis.

GaitGuard Performance Metrics. We evaluated *GaitGuard*’s runtime performance in a live collaborative setting. On the HoloLens 2, optimal application experience requires an app frame rate of 60 fps [49], while Mixed Reality Capture (MRC) typically achieves 30 fps for camera streaming [48]. We measured how mitigation processing described in Section 6 affects application and streaming frame rates, under varying temporal configurations (static vs. adaptive modes).

7.2 Mitigation Aspects Ablation Study

This section analyzes the impact of various mitigation aspects on privacy and utility metrics in 248 tested configurations. We evaluate how each aspect affects the system’s effectiveness by averaging metrics between users, box sizes, mitigation types, and parameters.

Effect of Mitigation Location (1). To evaluate the impact of different spatial locations, we calculated the mean values of each metric per location configuration, summarized in Table 1. Results

Table 1: Privacy and Utility Metrics for Different Mitigation Locations.

Mitigation Location	Average SSIM	Average PSNR	Average JSD	Reduction in Prof. Accuracy (%)
KPM	0.957	32.060	0.408	8.9
Head and Shoulders KPM	0.958	32.850	0.456	6.9
Lower body KPM	0.955	32.349	0.495	19.9
All except head KPM	0.942	31.418	0.504	22.2
LBM	0.925	24.835	0.580	56.6

Table 2: Privacy and Utility Metrics for Different Masking Box Sizes

Box Size (px)	Average SSIM	Average PSNR	Average JSD	Reduction in Prof. Accuracy (%)
50	0.979	35.193	5.167	0.457
100	0.955	31.430	21.889	0.478
150	0.926	29.163	24.032	0.489
200	0.926	28.037	20.634	0.457

show that baseline KPM and head & shoulders KPM configurations achieved high utility (SSIM ≈ 0.96 , PSNR ≈ 32 dB) but minimal privacy impact (< 10% reduction in gait profiling accuracy, JSD: 0.40–0.45). This suggests that targeting a few keypoints inadequately protects gait privacy, possibly due to OpenPose’s ability to interpolate obscured keypoints via part affinity fields [7]. Lower body KPM and all-except-head KPM, on the other hand, showed improved privacy metrics ($\approx 20\%$ reduction in gait profiling accuracy, JSD ≈ 0.50). Lower body KPM offered marginally better utility (SSIM and PSNR gains < 3%) and slight improvements in privacy. This suggests that obfuscating additional lower body joints enhances privacy protection, while expanding beyond the lower body yields minimal additional benefit. LBM (Lower Body Masking) delivered the strongest privacy performance (56.6% reduction in gait profiling accuracy, highest JSD: 0.58), indicating a substantial distortion of gait-relevant information. However, it also showed the lowest utility (SSIM: 0.925, PSNR: 24.8dB), highlighting the privacy–utility trade-off.

In summary, these results emphasize the importance of targeting lower body regions to protect gait privacy. Relying solely on a few standard keypoints is insufficient, and although broader masking can further improve privacy, the gains may not justify the increased utility loss. LBM offers the most gait privacy protection, but incurs the highest visual degradation.

Effect of Mitigation Size (2). Next, we analyze how the size of the mitigation mask influences privacy protection and visual quality. The average results for each box size tested are summarized in Table 2. Values are aggregated across all users, mitigation types, locations, and parameters.

Smaller box sizes (e.g., 50 pixels) preserved the highest visual quality (SSIM: 0.979, PSNR: 35.19 dB) but offered the least privacy protection (lowest JSD: 0.457, reduction in gait profiling accuracy: 5.17%). However, increasing the size of the box improved privacy. The 100-pixel masks reduced gait profiling accuracy by 21.89% (JSD: 0.478) with moderate utility decline (SSIM: 0.955). Interestingly, the 150-pixel configuration achieved best privacy (highest JSD: 0.489, 24.03% accuracy reduction) while maintaining acceptable visual quality (SSIM: 0.926). Increasing the mask size to 200 pixels did not further improve privacy. Despite a lower PSNR (28.04 dB), JSD decreased to 0.457, and the reduction in gait profiling accuracy

Table 3: Privacy and Utility Metrics for Different Mitigation Types

Type	Average SSIM	Average PSNR	Average JSD	Reduction in Prof. Accuracy (%)
Black box	0.930	23.570	0.516	31.915
DP Pix	0.942	19.804	0.541	39.966
DP Laplace	0.951	32.843	0.468	15.373
Blur	0.981	37.865	0.380	4.492
Uniform	0.958	34.167	0.441	20.103
Normal	0.951	31.687	0.461	25.852
Laplace	0.946	30.577	0.469	27.830
Exponential	0.950	28.084	0.466	25.474
Average Color	0.961	29.782	0.503	32.626

fell to 20.63%. This suggests diminishing returns beyond a threshold, possibly due to excessive overlap with non-informative regions.

These results demonstrate that the mask size is a key factor in balancing privacy and utility. A 150-pixel box appears to offer the most favorable trade-off, with strong privacy gains and manageable visual distortion.

Effect of Mitigation Type (3). The performance of each mitigation type is summarized in Table 3. The values presented were averaged for all users, locations, box sizes, and parameter settings.

The baseline black box method offers the strongest privacy metrics among simpler techniques (31.92% reduction in gait profiling accuracy, JSD: 0.516), but it causes significant visual distortion with the lowest SSIM (0.93) and second lowest PSNR (23.57 dB), suggesting the need for more nuanced alternatives.

Random noise methods (uniform, normal, Laplace, exponential) showed consistent results: moderate privacy protection (JSD: 0.441–0.469, reduction in gait profiling accuracy: 20.1–27.8%) with better utility than black box (SSIM: 0.946 – 0.958, PSNR ≤ 34.17 dB). This indicates that noise-based perturbations offer a balanced privacy–utility trade-off, without surpassing the baseline’s privacy effectiveness. DP Laplace method performed similarly to noise-based approaches (JSD: 0.468, 15.37% reduction in gait profiling accuracy) with strong utility (SSIM: 0.951, PSNR: 32.84 dB). However, it did not offer a better privacy–utility balance than simpler noise techniques. In contrast, despite its popularity, Gaussian blur showed the weakest privacy performance (lowest JSD: 0.380, 4.49% reduction in gait profiling accuracy), indicating ineffectiveness in concealing gait characteristics. However, it best preserved the image quality (SSIM: 0.981, PSNR: 37.87 dB).

Two mitigation types, DP Pix and Average Color, stood out for delivering strong privacy protection. DP Pix achieved the highest JSD (0.541) and gait profiling accuracy reduction (39.97%), but lower utility (SSIM: 0.942, PSNR: 19.80 dB). Average Color offered better balance: 32.63% accuracy reduction, JSD of 0.503, with higher utility (SSIM: 0.961, PSNR: 29.78 dB).

Among all the methods evaluated, only three—black box, DP Pix, and Average Color—produced significantly altered gait feature distributions (JSD > 0.5). Of these, Average Color offered the most compelling privacy–utility trade-off, making it a strong candidate for real-time deployment in MR environments.

7.3 Adaptive Mitigation Results

To assess the impact of temporal adaptation in mitigation, we compared the performance of mitigation applied to every frame (static

Table 4: Comparison of Dynamic and Static Mitigation Methods

Type	Temporal	Ave. SSIM	Ave. PSNR	Reduction in Prof. Accuracy	Ave. JSD
Black Box	Static	0.89	20.93	68%	0.63
Ave. Color	Static	0.95	23.24	68%	0.63
Black Box	Adaptive	0.95	23.5	68%	0.63
Ave. Color	Adaptive	0.97	28.86	68%	0.63

mitigation) and mitigation applied to key frames representing gait events (adaptive mitigation) using representative configurations. Specifically, we selected the LBM location (Lower Body Masking) paired with two mitigation types: the baseline black box and the top-performing average color method.

The results, summarized in Table 4, show that the privacy metrics remained consistent in all configurations—each approach resulted in a 68% reduction in gait profiling accuracy and a JSD score of 0.63. However, notable improvements in visual quality were observed with adaptive mitigation. For both black box and average color, adaptive mitigation increased SSIM and PSNR values compared to their static counterparts. The average color method, in particular, saw the highest utility gain: SSIM improved from 0.95 to 0.97, and PSNR increased from 23.24 dB to 28.86 dB. This improvement can be attributed to the selective application of mitigation to gait-relevant frames (e.g., around heel-strike and toe-off events), reducing unnecessary distortion in noninformative frames.

These findings highlight the benefits of adaptive mitigation, which maintains privacy efficacy while improving visual quality. This makes it especially valuable for real-time MR applications, where preserving the user experience is critical.

7.4 Summary of Privacy-Utility Trade-offs

We evaluated the privacy-utility trade-offs (PUT) of all 248 mitigation configurations by comparing the accuracy of user gait profiling (privacy) against two standard utility metrics: PSNR and SSIM. The results, visualized in Table 5, reveal key findings in mitigation types, locations, and parameter choices.

Average color mitigation at the lower body KPM location achieved the best overall performance, producing the highest PSNR and SSIM while maintaining maximum observed privacy (68% reduction in gait profile accuracy). A close second was the same mitigation type at the LBM location, with equivalent privacy but slightly lower utility (1.8 dB lower PSNR, 0.003 decrease in SSIM). Average color consistently offered the best privacy-utility trade-off across all mitigation types. In contrast, the black box method, while equally effective in reducing gait profiling accuracy, produced significantly worse utility results.

Mitigation applied only to the three gait-related keypoints in the baseline KPM proved insufficient. OpenPose compensates for missing keypoints by inferring positions from surrounding body parts, reducing the impact on privacy. The improved performance of the head & shoulders KPM configuration, which mitigates additional non-gait keypoints, further supports this, as it disrupts OpenPose’s estimation process more effectively. Applying DP pixelization and average color to either LBM or lower body KPM location with a 150-pixel box size resulted in nearly identical privacy and utility

outcomes. This suggests that with sufficiently large masked regions, keypoint-based mitigation can approximate the coverage and effectiveness of full lower-body masking.

Finally, adaptive mitigation strategies provided privacy metrics comparable to their static counterparts while significantly improving utility. By focusing mitigation on gait-critical frames (e.g., during heel-strike and toe-off), adaptive methods reduce unnecessary visual distortion, making them ideal for deployment in real-time MR systems.

7.5 Effectiveness of *GaitGuard* Across Multiple Gait Analysis Methods

Our mitigation experiments identified that applying average color at the LBM location is among the most effective strategies to protect gait information. Both static and adaptive applications of this configuration yielded comparable privacy outcomes. To further evaluate the generalizability of the effectiveness of *GaitGuard*, we tested its performance using static configuration against two state-of-the-art video-based gait analysis methods.

The first method follows a numerical approach to gait analysis based on pose estimation by Stenum et al. [76], which we automated as *GaitExtract* (see Section 4.3). The second method, GaitLab [29], employs deep neural networks to extract gait features from video input. As shown in Table 6, *GaitGuard* significantly reduced the accuracy of gait profiling between both analysis methods. Specifically, *GaitExtract* recorded a reduction of 64%, while GaitLab showed a reduction of 36%. These results indicate that *GaitGuard* effectively obfuscates gait characteristics, regardless of whether the analysis method is based on hand-engineered features or learned neural representations.

Jensen-Shannon divergence (JSD) scores further highlight the degree of alteration in gait feature distributions post-mitigation. *GaitExtract* recorded a high average JSD of 0.63, suggesting substantial deviation, while GaitLab showed a moderate change (JSD = 0.22), consistent with its partially opaque internal representation. Importantly, both systems exhibited statistically significant differences in the gait feature distributions before and after mitigation, as confirmed by the Mann-Whitney U test.

These results underscore the robustness of *GaitGuard*’s mitigation capabilities across diverse gait analysis pipelines. By effectively disrupting both traditional and neural network-based gait models—without compromising utility—*GaitGuard* establishes itself as a practical, general-purpose solution for preserving gait privacy in real-world MR deployments.

7.6 System Performance

We summarize *GaitGuard*’s real-time system performance, comparing static and adaptive temporal configurations while applying average color mitigation at the LBM location. Furthermore, we evaluate the effect of varying the depth of ConvNet explained in Section 4.4 for the adaptive configuration, as summarized in Table 7.

Figure 8 visualizes the impact of these configurations on application and streaming frame rates. The bar graph shows that all setups maintain a high application FPS (52–54), indicating that *GaitGuard* introduces negligible overhead on MR app responsiveness. For streaming, both the static configuration and the adaptive

Table 5: The privacy-utility tradeoff (PUT) of all mitigation techniques using gait features from the fully automated *GaitExtract*. The privacy metric (reduction in gait profiling accuracy) was compared with two different utility metrics: (1) PSNR and (2) SSIM.

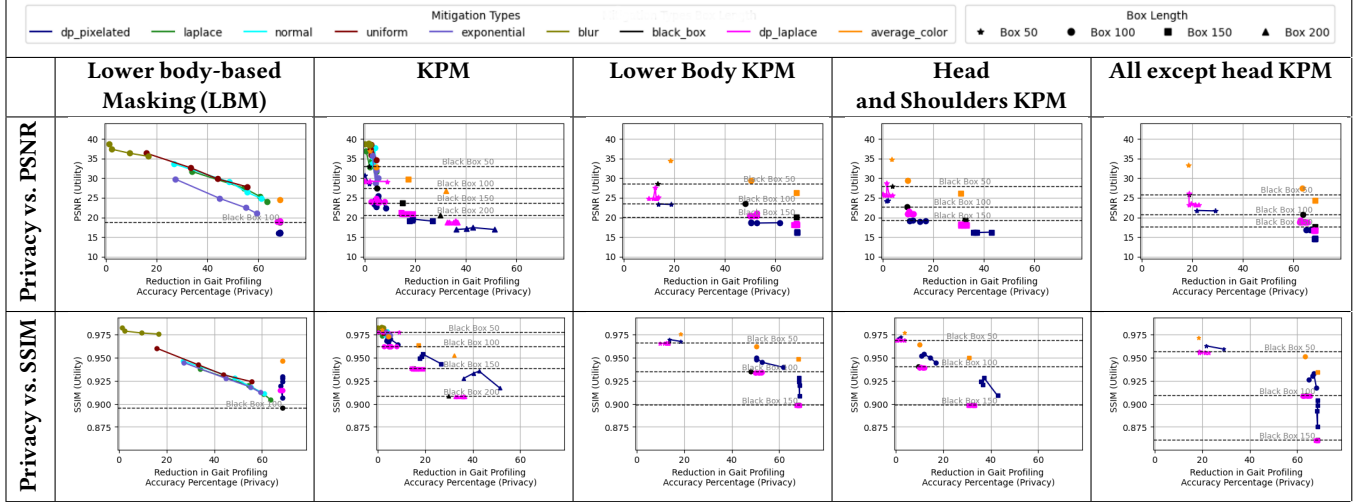


Table 6: *GaitGuard* Performance on State-of-the-Art Video-based Gait Analysis Methods

	<i>GaitExtract</i>	<i>Gait Lab</i> [29]
Reduction in Prof. Accuracy	64%	36%
Average JSD	0.63	0.22
Significantly Different? (U-test)	Yes	Yes

Table 7: Evaluation Metrics for Static and Adaptive Mitigation

	Approx. Application FPS	Approx. Streaming FPS	Gait Event Recall (%)	Average SSIM	Average PSNR
Static	52	29	N/A	0.95	23.50
1 Layer	53	29	95.60	0.97	28.69
2 Layers	53	28	96.69	0.97	28.99
3 Layers	54	12	91.67	0.97	29.02
4 Layers	52	10	95.12	0.97	27.89
5 Layers	53	8	94.30	0.97	28.98

model with one convolution layer maintain 29 FPS, demonstrating compatibility with real-time MR rendering and capture pipelines.

As model depth increases, streaming FPS drops significantly, falling to 28 with two layers, then declining sharply to 12, 10, and 8 FPS for three, four, and five layers, respectively. This illustrates a clear trade-off between model complexity and system throughput. Despite this drop in streaming performance, all adaptive configurations with 1–5 layers achieved over 90% gait event recall. The five-layer model produced 95% recall and a 64% reduction in gait profiling accuracy (JSD = 0.63), showing strong privacy protection. However, since simpler models offer similar privacy with far better streaming efficiency, one convolution layer suffices in this setting.

These results suggest that deeper gait event models may be useful in more challenging environments (e.g., noisy or occluded scenes) but are unnecessary for typical indoor MR use. In general, *GaitGuard* effectively protects gait privacy while preserving frame rate and user experience.

7.7 Scalability

Although some MR platforms are technically capable of hosting larger gatherings, a closer look at common applications reveals that the typical number of participants actively collaborating in a shared MR session generally does not exceed five. Many highly effective use cases, particularly in enterprise settings like remote assistance (Dynamics 365 Remote Assist [55]), detailed design review (Trimble Connect [80]), and focused creative work (Gravity Sketch [72]), are explicitly designed for or naturally suited to very small groups of 1–5 users. This limitation often stems from the need for high-fidelity interaction with complex 3D data, clear communication pathways, manageable cognitive load, and maintaining application performance, all of which become significantly more challenging as the number of participants increases in an immersive environment. Furthermore, previous work highlights that most group behavior studies in MR tend to focus on groups of 3–6 members, with four being particularly common due to the natural constraint of human conversation dynamics and social coordination [31, 40, 69]. Therefore, despite the potential for larger virtual meetings or events on platforms like Workrooms, Mesh, or Spatial, the most prevalent and practical applications of deep, interactive MR collaboration currently revolve around these smaller, more focused group sizes. More details on some of these applications are provided in Table 8.

To quantify *GaitGuard*'s scalability performance with increasing participants and multiple viewpoints, we analyzed two scenarios: one with 2–4 people (typical for collaborative MR applications) and another with 10+ people (representing an extreme case), where participants are positioned at different angles within the camera's field of view.

Results are summarized in Table 9, showing that for 2–4 people, *GaitGuard* maintains reasonable performance. The static configuration and 1-layer adaptive model achieve 25 and 21 FPS, respectively, close to the minimum acceptable streaming rate of 24 FPS [56]. This indicates effective handling of small group collaborations without significant performance degradation. With 10+ people, performance decreases in all configurations. Static and 1-layer models

Table 8: Collaborative MR Applications

App / Product ^a	Typical Users	Primary Use Case
Dynamics 365 Guides [53]	1 (+1 expert)	Solo holographic workflow; optional 1-on-1 remote help.
Dynamics 365 Remote Assist [55]	2	“See-what-I-see” remote support (field tech ↔ expert).
Microsoft Mesh [54]	2–16+	Immersive meetings; cap varies by scenario.
Trimble Connect [80]	2–5	Small-team review of complex models on-site.
Meta Horizon Workrooms [45]	≤ 16 VR (+≈ 50 video)	VR meetings with video dial-in overflow.
Meta Horizon Worlds [46]	4–40+	Social VR spaces; limit set by world complexity.
Spatial [74]	5–50+	Cross-platform meetings/events; plan-based tiers.
Arthur [3]	2–30	Enterprise virtual office / workshops.
Engage [17]	10–100 s	Classes, lectures, large-scale events.
Gravity Sketch [72]	2–8	Collaborative 3-D design/modeling.

^a Some listed apps may be deprecated.

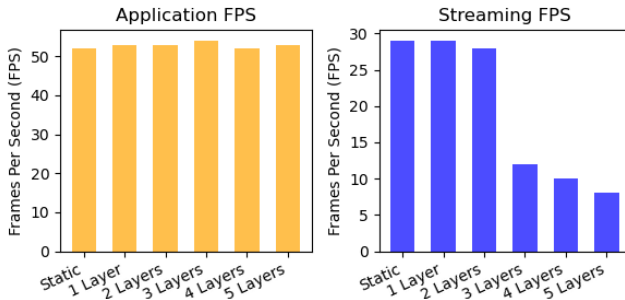


Figure 8: Performance comparison across static and adaptive configurations. Application FPS remains consistent (52–54), while streaming FPS decreases with model depth, showing the trade-off between complexity and efficiency.

Table 9: Stream FPS with Multiple Participants & Viewpoints

	Stream FPS (> 10 ppl.)	Stream FPS (2–4 ppl.)
Adaptive	Static	18
	1 Layer	17
	2 Layers	12
	3 Layers	8
	4 Layers	7
	5 Layers	7

maintain the highest frame rates (18 and 17 FPS), which may suffice for some applications but fall short of real-time standards. Deeper models show similar performance across both scenarios, suggesting that model complexity, rather than scene occupancy, is the primary performance bottleneck.

These results demonstrate that *GaitGuard* scales well for small group collaborations, which comprise most practical MR applications. For larger gatherings, further optimization may be necessary to achieve privacy protection and real-time performance.

7.8 Qualitative Evaluation

To better understand user perceptions of gait privacy and evaluate the subjective effectiveness of *GaitGuard*, we conducted a two-part

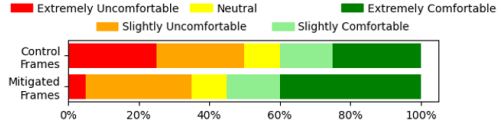
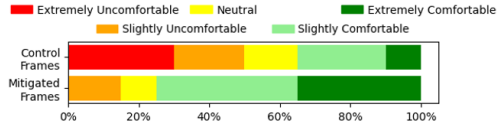
Before being informed about gait privacy concerns and GaitGuard performance**After being informed about gait privacy concerns and GaitGuard performance**

Figure 9: The Likert responses for the gait privacy perception survey were distributed across unmodified and mitigated frames with *GaitGuard*.

user study with 20 participants. The cohort was balanced, comprising individuals with and without prior VR/MR experience, to capture a range of privacy perspectives.

Participants completed a structured questionnaire that assessed their comfort level in sharing video frames before and after mitigation. The first part of the study asked participants to rate their comfort in sharing unaltered and *GaitGuard* processed egocentric video frames using a 5-point Likert scale (1 = extreme discomfort, 5 = extreme comfort). As shown in Figure 9, 50% of the participants expressed discomfort in sharing unmitigated gait video, while 40% reported comfort. After viewing frames processed with *GaitGuard*, comfort levels rose to 65%, indicating that privacy-preserving transformations can improve user acceptance.

In the second phase, participants were informed about the privacy risks associated with gait data in MR, including the inference of sensitive attributes such as ethnicity, age, gender, and neuromusculoskeletal health conditions. They were also briefed on the performance of *GaitGuard*, including its ability to reduce the accuracy of gait profiling from 78% to 16%, with only a 0.123-second processing delay and without affecting the egocentric view. After this information, comfort with sharing unchanged frames decreased, reflecting increased risk awareness. However, 35% remained comfortable with raw footage, while 75% reported comfort in sharing *GaitGuard* processed video.

These findings suggest that technological interventions and risk awareness shape user perceptions of gait privacy. Although *GaitGuard* substantially improves perceived and actual privacy, the study highlights the importance of transparency and informed consent. Participants favored solutions that provided strong privacy guarantees without degrading the system’s utility. The results support *GaitGuard* as a practical and user-aligned approach to protecting gait privacy in MR environments.

8 Practical Recommendations

Our evaluation of 248 mitigation configurations reveals key insights for MR system designers:

- **Target Lower Body Mitigation.**

Lower body masking (LBM) significantly outperform isolated keypoint approaches, achieving a 68% reduction in gait profiling accuracy.

- **Use Average Color Masking.**

This technique provides optimal privacy-utility balance without substantial image degradation, unlike black boxes or heavy noise.

- **Utilize Adaptive Mitigation**

Spatial awareness improves image quality (PSNR/SSIM) without sacrificing privacy by targeting gait-critical frames.

- **Keep Detection Models Simple.** One convolutional layer suffices for gait event detection—deeper models reduce streaming performance without privacy gains.

- **Communicate Risks to Build User Trust.** Participants expressed greater comfort and trust after being informed about gait privacy risks and mitigation techniques. This highlights the importance of transparency, education, and user agency in privacy-preserving MR system design.

- **Additional Utility Metrics.** Although we considered general application-agnostic utility metrics for image quality, including SSIM and PSNR, other application-based utility measures could be added to *GaitGuard* accordingly.

- **Practical Applicability.** Deploying gait-privacy countermeasures as an OS-level service on the headset would minimize latency and maximize control. Current mixed-reality platforms (e.g., HoloLens 2) provide limited compute and only high-level camera access, making real-time, on-device transformations impractical. Future generations of head-mounted devices (HMDs) will likely offer greater processing capacity and lower-level APIs, paving the way for effective on-device privacy protection.

Key Takeaway: Simple approaches work. *GaitGuard* demonstrates that practical, real-time gait privacy is achievable using lightweight, interpretable, and non-adversarial methods. By avoiding resource-intensive solutions such as GANs or adversarial perturbations, *GaitGuard* strikes an effective balance between usability, deployability, and privacy protection, making it an ideal candidate for MR platforms deployed in everyday environments. Although our evaluation was conducted in controlled indoor settings, future work may explore robustness in more diverse environments.

9 Conclusion

We presented *GaitGuard*, a real-time system to mitigate risks to gait privacy in MR environments. Designed for compatibility with commercial MR platforms, *GaitGuard* applies targeted mitigation strategies—most effectively, average color masking to lower-body regions—to protect against video-based gait profiling while maintaining high visual quality.

Across 248 configurations tested, *GaitGuard* consistently achieved strong privacy results, reducing the accuracy of gait profiling by up to 68% with users' accepted performance overhead. Adaptive mitigation further improved utility by selectively applying protection at gait-critical moments. Importantly, our findings show that simple and interpretable methods - rather than complex adversarial or generative techniques - are sufficient to achieve robust gait privacy in practice.

GaitGuard runs in real-time, integrates easily with collaborative MR workflows, and is deployable on commodity hardware.

Acknowledgments

This research was partially supported by NSF awards 2339266 and 1956393, and a gift from the Noyce Initiative.

References

- [1] Paariaat Aditya, Rijurekha Sen, Peter Druschel, Seong Joon Oh, Rodrigo Benenson, Mario Fritz, Bernt Schiele, Bobby Bhattacharjee, and Tong Tong Wu. 2016. I-pic: A platform for privacy-compliant image capture. In *Proceedings of the 14th annual international conference on mobile systems, applications, and services*. Association for Computing Machinery, New York, NY, USA, 235–248.
- [2] Apple. 2023. Apple Vision Pro.
- [3] Arthur. 2025. Arthur. <https://arthur.digital>.
- [4] Richard Baker, Alberto Esquenazi, Maria Grazia Benedetti, Kaat Desloovere, et al. 2016. Gait analysis: clinical facts. *Eur. J. Phys. Rehabil. Med* 52, 4 (2016), 560–574.
- [5] Olivier Beauchet, Cédric Annweiler, Michele L Callisaya, Anne-Marie De Cock, Jorunn L Helbostad, Reto W Kressig, Velandai Srikanth, Jean-Paul Steinmetz, Helena M Blumen, Joe Vergheese, et al. 2016. Poor gait performance and prediction of dementia: results from a meta-analysis. *Journal of the American Medical Directors Association* 17, 6 (2016), 482–490.
- [6] Z. Cao, G. Hidalgo Martinez, T. Simon, S. Wei, and Y. A. Sheikh. 2019. OpenPose: Realtime Multi-Person 2D Pose Estimation using Part Affinity Fields.
- [7] Zhe Cao, Tomas Simon, Shih-En Wei, and Yaser Sheikh. 2017. Realtime Multi-Person 2D Pose Estimation Using Part Affinity Fields. In *Proceedings of the IEEE Conference on Computer Vision and Pattern Recognition (CVPR)*.
- [8] Aurelio Cappozzo. 1984. Gait analysis methodology. *Human movement science* 3, 1-2 (1984), 27–50.
- [9] Yasra Chandio and Fatima M. Anwar. 2020. Spatiotemporal security in mixed reality systems. In *Proceedings of the 18th Conference on Embedded Networked Sensor Systems (Virtual Event, Japan) (SenSys '20)*. Association for Computing Machinery, New York, NY, USA, 725–726.
- [10] Kaiming Cheng, Jeffery F Tian, Tadayoshi Kohno, and Franziska Roesner. 2023. Exploring user reactions and mental models towards perceptual manipulation attacks in mixed reality. In *USENIX Security*, Vol. 18.
- [11] Ruizhi Cheng, Nan Wu, Vu Le, Eugene Chai, Matteo Varvello, and Bo Han. 2024. Magicstream: Bandwidth-conserving immersive telepresence via semantic communication. In *Proceedings of the 22nd ACM Conference on Embedded Networked Sensor Systems*. 365–379.
- [12] Guglielmo Cola, Marco Avvenuti, Fabio Musso, and Alessio Vecchio. 2016. Gait-based authentication using a wrist-worn device. In *Proceedings of the 13th International Conference on Mobile and Ubiquitous Systems: Computing, Networking and Services*. 208–217.
- [13] Matthew Corbett, Brendan David-John, Jiacheng Shang, Y Charlie Hu, and Bo Ji. 2023. BystandAR: Protecting Bystander Visual Data in Augmented Reality Systems. In *Proceedings of the 21st Annual International Conference on Mobile Systems, Applications and Services*. 370–382.
- [14] Paula Delgado-Santos, Ruben Tolosana, Richard Guest, Ruben Vera-Rodriguez, Farzin Deravi, and Aytahmi Morales. 2022. GaitPrivacyON: Privacy-preserving mobile gait biometrics using unsupervised learning. *Pattern Recognition Letters* 161 (2022), 30–37.
- [15] Paula Delgado-Santos, Ruben Tolosana, Richard Guest, Ruben Vera-Rodriguez, Farzin Deravi, and Aytahmi Morales. 2022. GaitPrivacyON: Privacy-preserving mobile gait biometrics using unsupervised learning. *Pattern Recognition Letters* 161 (Sept. 2022), 30–37.
- [16] Mohammad O Derawi, Patrick Bours, and Kjetil Holien. 2010. Improved cycle detection for accelerometer based gait authentication. In *2010 Sixth International Conference on Intelligent Information Hiding and Multimedia Signal Processing*. IEEE, 312–317.
- [17] Engage. 2025. Engage. <https://engagevr.io>.
- [18] Photon Engine. 2023. Photon Unity Networking for Unity Multiplayer Games PUN2. <https://www.photonengine.com/PUN>.
- [19] Liyue Fan. 2018. Image pixelization with differential privacy. In *Data and Applications Security and Privacy XXXII: 32nd Annual IFIP WG 11.3 Conference, DBSec 2018, Bergamo, Italy, July 16–18, 2018, Proceedings* 32. Springer, 148–162.
- [20] Habiba Farrukh, Reham Mohamed, Aniket Nare, Antonio Bianchi, and Z Berkay Celik. 2023. {LocIn}: Inferring Semantic Location from Spatial Maps in Mixed Reality. In *32nd USENIX Security Symposium (USENIX Security 23)*. 877–894.
- [21] Moshe Gabel, Ran Gilad-Bachrach, Erin Renshaw, and Assaf Schuster. 2012. Full body gait analysis with Kinect. In *2012 Annual International Conference of the IEEE Engineering in Medicine and Biology Society*. IEEE, 1964–1967.
- [22] Davrondzhon Gafurov, Einar Snekkens, and Patrick Bours. 2007. Gait authentication and identification using wearable accelerometer sensor. In *2007 IEEE workshop on automatic identification advanced technologies*. IEEE, 220–225.
- [23] Mar Gonzalez-Franco, Rodrigo Pizarro, Julio Cermeron, Katie Li, Jacob Thorn, Windo Hutabarat, Ashutosh Tiwari, and Pablo Bermell-Garcia. 2017. Immersive Mixed Reality for Manufacturing Training. *Frontiers in Robotics and AI* 4 (Feb. 2017).
- [24] Amira Guesmi, Khaled N Khasawneh, Nael Abu-Ghazaleh, and Ihsen Alouani. 2022. Room: Adversarial machine learning attacks under real-time constraints.

In 2022 International Joint Conference on Neural Networks (IJCNN). IEEE, 1–10.

[25] Simon Hanisch, Evelyn Muschter, Admantini Hatzipanayioti, Shu-Chen Li, and Thorsten Strufe. 2023. Understanding Person Identification Through Gait. *Proceedings on Privacy Enhancing Technologies* 2023, 1 (Jan. 2023), 177–189.

[26] Ismat Jarin, Yu Duan, Rahmadi Trimananda, Hao Cui, Salma Elmalaiki, and Athina Markopoulou. 2023. BehaVR: User Identification Based on VR Sensor Data. *arXiv preprint arXiv:2308.07304* (2023).

[27] Jk Jensen, Jinhan Hu, Amir Rahmati, and Robert LiKamWa. 2019. Protecting Visual Information in Augmented Reality from Malicious Application Developers. In *The 5th ACM Workshop on Wearable Systems and Applications* (Seoul, Republic of Korea) (*WearSys ’19*). Association for Computing Machinery, New York, NY, USA, 23–28.

[28] Glenn Jocher et al. 2020. YOLOv5 by Ultralytics. <https://github.com/ultralytics/yolov5>.

[29] Lukasz Kidzinski, Bryan Yang, Jennifer L. Hicks, Apoorva Rajagopal, Scott L. Delp, and Michael H. Schwartz. 2020. Deep neural networks enable quantitative movement analysis using single-camera videos. *Nature Communications* 11, 1 (Aug. 2020). <https://www.nature.com/articles/s41467-020-17807-z>

[30] YoungIn Kim, Seokhyun Hwang, Jeongseok Oh, and Seungjim Kim. 2024. GaitWay: Gait Data-Based VR Locomotion Prediction System Robust to Visual Distraction. In *Extended Abstracts of the CHI Conference on Human Factors in Computing Systems* (Honolulu, HI, USA) (*CHI EA ’24*). Association for Computing Machinery, New York, NY, USA, Article 173, 8 pages.

[31] Jaime Arona Krems and Jason Wilkes. 2019. Why are conversations limited to about four people? A theoretical exploration of the conversation size constraint. *Evolution and Human Behavior* 40, 2 (2019), 140–147.

[32] Sudhakar Kumawat and Hajime Nagahara. 2022. Privacy-Preserving Action Recognition via Motion Difference Quantization. In *European Conference on Computer Vision*. Springer, 518–534.

[33] California State Legislature. 2013. The CPRA.

[34] Rui Li, Tianwei Li, Rui Zhang, Yinqian Li, Xinyu Wang, and Yinzh Li. 2024. Speak Up, I’m Listening: Extracting Speech from Zero-Permission VR Sensors. In *Proc. of the Network and Distributed System Security Symposium (NDSS)*.

[35] Wenwei Li, Ruofeng Liu, Shuai Wang, Dongjiang Cao, and Wenchao Jiang. 2023. Egocentric human pose estimation using head-mounted mmwave radar. In *Proceedings of the 21st ACM Conference on Embedded Networked Sensor Systems*. 431–444.

[36] Qi Lin, Yisheng Cui, Shanqing Jiang, Tengyu Ma, Weitao Xu, and Wen Hu. 2017. Automatic Key Generation Using Motion Energy Harvesters. In *NDSS Symposium 2017*.

[37] Tsung-Yi Lin, Priya Goyal, Ross Girshick, Kaiming He, and Piotr Dollár. 2017. Focal loss for dense object detection. In *Proceedings of the IEEE International Conference on Computer Vision*. 2980–2988.

[38] Rationalstat LLC. 2023. Mixed Reality Market Is Set to Double by 2030. <https://www.globenewswire.com/news-release/2023/09/22/2747789/0/en/Mixed-Reality-Market-is-Set-to-Double-by-2030-Mixed-Reality-Market-Share-Size-Growth-Forecast-2023-2030-RationalStat-Study.html>.

[39] Luca Lonini, Yaejin Moon, Kyle Embry, R James Cotton, Kelly McKenzie, Sophia Jenz, and Arun Jayaraman. 2022. Video-based pose estimation for gait analysis in stroke survivors during clinical assessments: a proof-of-concept study. *Digital Biomarkers* 6, 1 (2022), 9–18.

[40] Paul Benjamin Lowry, Tom L Roberts, Nicholas C Romano Jr, Paul D Cheney, and Ross T Hightower. 2006. The impact of group size and social presence on small-group communication: Does computer-mediated communication make a difference? *Small group research* 37, 6 (2006), 631–661.

[41] Wei Luo, Jianhao Xu, Shouling Zhu, Rui Wang, and Peng Liu. 2023. Eavesdropping on Controller Acoustic Emanation for Keystroke Inference Attack in Virtual Reality. In *Proc. of the Network and Distributed System Security Symposium (NDSS)*.

[42] Martina Mancini and Fay B Horak. 2010. The relevance of clinical balance assessment tools to differentiate balance deficits. *European journal of physical and rehabilitation medicine* 46, 2 (2010), 239.

[43] Meta. 2023. Meta Quest 3: Mixed Reality VR Headset. <https://www.meta.com/quest/quest-3/>.

[44] Meta. 2024. Introducing Project Aria from Meta. <https://www.projectaria.com>

[45] Meta. 2025. Meta Horizon Workrooms. <https://forwork.meta.com/horizon-workrooms/>.

[46] Meta. 2025. Meta Horizon Worlds. <https://www.meta.com/experiences/worlds/2532035600194083/>.

[47] Microsoft. 2022. Introduction to the Multi-user Capabilities Tutorials - Mixed Reality. <https://learn.microsoft.com/en-us/windows/mixed-reality/develop/unity/tutorials/mr-learning-sharing-01>.

[48] Microsoft. 2022. Mixed Reality Capture Overview. <https://learn.microsoft.com/en-us/windows/mixed-reality/develop/advanced-concepts/mixed-reality-capture-overview>.

[49] Microsoft. 2022. Performance - MRTK 2. <https://learn.microsoft.com/en-us/windows/mixed-reality/mrtk-unity/mrtk2/performance/perf-getting-started?view=mrtkunity-2022-05>.

[50] Microsoft. 2023. HoloLens 2 Hardware. <https://learn.microsoft.com/en-us/hololens/hololens2-hardware>.

[51] Microsoft. 2023. HoloLens Microsoft 2. <https://www.microsoft.com/en-us/hololens/>.

[52] Microsoft. 2023. What Is Mixed Reality? <https://learn.microsoft.com/en-us/windows/mixed-reality/discover/mixed-reality>.

[53] Microsoft. 2025. Dynamics 365 Field Service. <https://www.microsoft.com/en-us/dynamics-365/products/field-service>.

[54] Microsoft. 2025. Microsoft Mesh. <https://www.microsoft.com/en-us/microsoft-teams/microsoft-mesh>.

[55] Microsoft. 2025. Remote Assist overview. <https://learn.microsoft.com/en-us/dynamics365/mixed-reality/remote-assist/ra-overview>.

[56] Lauren Milazzo. 2021. A production expert’s guide to frame rates and FPS. <https://vimeo.com/blog/post/fps-for-live-streaming>

[57] Anat Mirelman, Paolo Bonato, Richard Camicioli, Terry D Ellis, Nir Giladi, Jamie L Hamilton, Chris J Hass, Jeffrey M Hausdorff, Elisa Pelosin, and Quincy J Almeida. 2019. Gait impairments in Parkinson’s disease. *The Lancet Neurology* 18, 7 (2019), 697–708.

[58] National Instruments. 2024. Structural Similarity Index - NI. https://www.ni.com/docs/en-US/bundle/ni-vision-concepts-help/page/structural_similarity_index.html

[59] OpenCV Contributors. 2023. OpenCV. https://docs.opencv.org/3.4/d5/d33/structcv_1_1HOGDescriptor.html.

[60] Ion PI Pappas, Milos R Popovic, Thierry Keller, Volker Dietz, and Manfred Morari. 2001. A reliable gait phase detection system. *IEEE Transactions on neural systems and rehabilitation engineering* 9, 2 (2001), 113–125.

[61] Alexandra Pfister, Alexandre M West, Shaw Bronner, and Jack Adam Noah. 2014. Comparative abilities of Microsoft Kinect and Vicon 3D motion capture for gait analysis. *Journal of medical engineering & technology* 38, 5 (2014), 274–280.

[62] Physiopedia. 2025. Gait Definitions. https://www.physio-pedia.com/Gait_Definitions.

[63] Walter Pirker and Regina Katzenschlager. 2017. Gait disorders in adults and the elderly: A clinical guide. *Wiener Klinische Wochenschrift* 129, 3 (2017), 81–95.

[64] Hari Prasanth, Miroslav Caban, Urs Keller, Grégoire Courtine, Auke Ijspeert, Heike Vallery, and Joachim Von Zitzewitz. 2021. Wearable sensor-based real-time gait detection: A systematic review. *Sensors* 21, 8 (2021), 2727.

[65] Kristina Prokopet and Romain Dupont. 2019. Towards Dense 3D Reconstruction for Mixed Reality in Healthcare: Classical Multi-View Stereo vs Deep Learning. In *Proceedings of the IEEE/CVF International Conference on Computer Vision (ICCV) Workshops*.

[66] Sanka Rasnayaka and Terence Sim. 2020. Your Tattletale Gait Privacy Invasiveness of IMU Gait Data. In *2020 IEEE International Joint Conference on Biometrics (IJCB)*. 1–10.

[67] Nisarg Raval, Animesh Srivastava, Ali Razeen, Kiron Lebeck, Ashwin Machanavajjhala, and Lanodn P. Cox. 2016. What You Mark is What Apps See. In *Proceedings of the 14th Annual International Conference on Mobile Systems, Applications, and Services* (Singapore, Singapore) (*MobiSys ’16*). Association for Computing Machinery, New York, NY, USA, 249–261.

[68] Diana Romero, Fatima Anwar, and Salma Elmalaiki. 2025. MoCoMR: A Collaborative MR Simulator with Individual Behavior Modeling. In *Proceedings of the 3rd International Workshop on Human-Centered Sensing, Modeling, and Intelligent Systems*. 114–119.

[69] Diana Romero, Yasra Chandio, Fatima Anwar, and Salma Elmalaiki. 2024. GroupBeaMR: Analyzing Collaborative Group Behavior in Mixed Reality Through Passive Sensing and Sociometry. *arXiv preprint arXiv:2411.05258* (2024).

[70] Zhiqi Shen, Shaojing Fan, Yongkang Wong, Tian-Tsung Ng, and Mohan Kankanhalli. 2019. Human-imperceptible Privacy Protection Against Machines. In *Proceedings of the 27th ACM International Conference on Multimedia (MM ’19)*. Association for Computing Machinery, New York, NY, USA, 1119–1128.

[71] Warit Sirichotdumrong and Hitoshi Kiya. 2021. A gan-based image transformation scheme for privacy-preserving deep neural networks. In *2020 28th European Signal Processing Conference (EUSIPCO)*. IEEE, 745–749.

[72] Gravity Sketch. 2025. Gravity Sketch. <https://gravitysketch.com>.

[73] Oulimene Sofuwa, Alice Nieuwboer, Kaat Desloovere, Anne-Marie Willem, Fabienne Chavret, and Ilse Jonkers. 2005. Quantitative gait analysis in Parkinson’s disease: comparison with a healthy control group. *Archives of physical medicine and rehabilitation* 86, 5 (2005), 1007–1013.

[74] Spatial. 2025. Spatial. <https://www.spatial.io>.

[75] Sruti Srinidhi, Edward Lu, Akul Singh, Saisha Kartik, Audi Lin, Tarana Laroia, and Anthony Rowe. 2025. An XR Platform that Integrates Large Language Models with the Physical World. In *Proceedings of the 23rd ACM Conference on Embedded Networked Sensor Systems*. 700–701.

[76] Jan Stenum, Cristina Rossi, and Ryan T Roemmich. 2021. Two-dimensional video-based analysis of human gait using pose estimation. *PLoS computational biology* 17, 4 (2021), e1008935.

[77] Mojtaba Taherisadr, Mohammad Abdullah Al Faruque, and Salma Elmalaiki. 2023. Erudite: Human-in-the-loop IoT for an adaptive personalized learning system. *IEEE Internet of Things Journal* (2023).

[78] TheTimes. 2014. Fan diagnosed Parkinson’s by chance, says Connolly. <https://www.thetimes.com/travel/destinations/australia-travel/australia/fan-diagnosed-parkinsons-by-chance-says-connolly-m2g98ml3pw2>.

[79] Florian Tramer and Dan Boneh. 2019. Adversarial training and robustness for multiple perturbations. *Advances in neural information processing systems* 32 (2019).

[80] Trimble. 2025. Trimble Connect for HoloLens. <https://www.trimble.com/en/products/building-construction-field-systems/connect-mr>.

[81] European Union. 2023. General Data Protection Regulation (GDPR). <https://gdpr-info.eu/>.

[82] Chris Warin and Delphine Reinhardt. 2022. Vision: Usable Privacy for XR in the Era of the Metaverse. In *Proceedings of the 2022 European Symposium on Usable Security*. 111–116.

[83] Chengshuo Xia, Atsuya Munakata, and Yuta Sugiura. 2023. Privacy-Aware Gait Identification With Ultralow-Dimensional Data Using a Distance Sensor. *IEEE Sensors Journal* 23, 9 (May 2023), 10109–10117.

[84] Weitao Xu, Yiran Shen, Yongtuo Zhang, Neil Bergmann, and Wen Hu. 2017. Gait-Watch: A Context-aware Authentication System for Smart Watch Based on Gait Recognition. In *Proceedings of the Second International Conference on Internet-of-Things Design and Implementation (IoTDI '17)*. Association for Computing Machinery, New York, NY, USA, 59–70.

[85] Youtube. 2024. Blur your videos - YouTube Help. <https://support.google.com/youtube/answer/9057652>.

[86] Shiqi Yu, Tieniu Tan, Kaiqi Huang, Kui Jia, and Xinyu Wu. 2009. A study on gait-based gender classification. *IEEE Transactions on image processing* 18, 8 (2009), 1905–1910.

[87] Michal Zajac, Konrad Zolna, Negar Rostamzadeh, and Pedro O Pinheiro. 2019. Adversarial framing for image and video classification. In *Proceedings of the AAAI Conference on Artificial Intelligence*, Vol. 33. 10077–10078.

[88] De Zhang, Yunhong Wang, and Bir Bhanu. 2010. Ethnicity classification based on gait using multi-view fusion. In *2010 IEEE Computer Society Conference on Computer Vision and Pattern Recognition-Workshops*. IEEE, 108–115.

[89] Ding Zhang, Puqi Zhou, Bo Han, and Parth Pathak. 2022. M5: Facilitating multi-user volumetric content delivery with multi-lobe multicast over mmWave. In *Proceedings of the 20th ACM Conference on Embedded Networked Sensor Systems*. 31–46.

[90] Jinrui Zhang, Deyu Zhang, Xiaohui Xu, Fucheng Jia, Yunxin Liu, Xuanzhe Liu, Ju Ren, and Yaoxue Zhang. 2020. MobiPose: Real-time multi-person pose estimation on mobile devices. In *Proceedings of the 18th Conference on Embedded Networked Sensor Systems*. 136–149.

[91] Rui Zhang, Rui Li, Yifan Xie, Yinzhi Li, and Kehuan Zhang. 2024. Non-intrusive and Unconstrained Keystroke Inference in VR Platforms via Infrared Side Channel. In *Proc. of the Network and Distributed System Security Symposium (NDSS)*.

[92] Xingwei Zhang, Xiaolong Zheng, and Wenji Mao. 2021. Adversarial perturbation defense on deep neural networks. *ACM Computing Surveys (CSUR)* 54, 8 (2021), 1–36.

[93] Yuhan Zhou, Robbin Romijnders, Clint Hansen, Jos van Campen, Walter Maetzler, Tibor Hortobágyi, and Claudine JC Lamoth. 2020. The detection of age groups by dynamic gait outcomes using machine learning approaches. *Scientific reports* 10, 1 (2020), 4426.

[94] Shunlin Zhu, Yulong Liu, Ziming Lin, Zhe Tang, and Ting Wang. 2024. SoundLock: A Novel User Authentication Scheme for VR Devices Using Auditory-Pupillary Response. In *Proc. of the Network and Distributed System Security Symposium (NDSS)*.

Received 20 February 2007; revised 12 March 2009; accepted 5 June 2009